Sensitivity of Psychophysical, Electrophysiological and Structural Tests for Detection and Progression Monitoring in Ocular Hypertension and Glaucoma

Miguel Raimundo[1,2]; Catarina Mateus[3]; Pedro Faria[1]; Bárbara Oliveiros[2]; João Cardoso[1]; João Filipe Silva[1]; José Moura Pereira[1]; Miguel Castelo-Branco[2]
[1] Ophthalmology Department, Centro Hospitalar e Universitário de Coimbra, Coimbra (CHUC), Portugal
[2] Visual Neuroscience Laboratory, IBILI - Institute of Biomedical Imaging and Life Sciences, Faculty of Medicine, University of Coimbra, Portugal
[3] Orthoptics Department, Escola Superior de Saúde do Instituto Politécnico do Porto, Portugal

ABSTRACT

Purpose: To characterize early visual impairment of patients in the glaucoma spectrum, using psychophysical, electrophysiological and structural methods.

Methods: Cohort of 52 patients, 18 patients with ocular hypertension (HT), 15 glaucoma suspects (GS) and 19 with primary open-angle glaucoma (G), and 20 age-matched controls. Quantitative psychophysical methods were used to assess magno (FDT, Frequency Doubling Technology), parvo and koniocellular pathways (Cambridge Color Test), and RGC function was assessed by Pattern Electroretinogram. RGC axonal thickness was obtained using OCT.

Results: Reduced mean achromatic contrast sensitivity ($p=0.0298$) was found in patients with HT, as well as a reduced PERG N-95 wave amplitude ($p=0.0499$). Chromatic thresholds were significantly increased for protan, deutan and tritan axes ($p<0.03$) in these patients when compared to controls. At approximately 80% specificity, FDT showed only moderate sensitivity to detect early functional damage (superior nasal, 66% sensitivity). The pattern of disease progression decline is approximately linear for all tests, but more severe in OCT, RNFL thickness ($R_a^2 = 0.47$).

Conclusion: We found relative damage of magno, parvo and koniocellular retinocortical pathways beginning in ocular hypertension. FDT and CCT Protan performed well in detecting early damage in ocular hypertension, whereas longitudinal analysis using OCT for RFNL appeared to be the best to monitor the progression. The sensitivity of currently available tests is lower comparing with our previously reported novel psychophysical tools (sensitivity above 90% for 80% specificity). We believe early diagnosis in glaucoma is possible by exploiting visual pathways with a small degree of redundancy through high sensitivity functional tests.

Keywords: Glaucoma, ocular hypertension, standard automated perimetry, optical coherence tomography, frequency doubling technology, pattern electroretinogram, color vision, magnocelullar, koniocellular, parvocelullar.

RESUMO

Objectivos: Caracterizar dano visual precoce no glaucoma, utilizando métodos psicofísicos, electrofisiológicos e estruturais.

Métodos: Coorte de 52 doentes, 18 com hipertensão ocular (HT), 15 suspeitos de glaucoma e 19 com glaucoma primário de ângulo aberto, e 20 controlos ajustados à idade. Foram utilizados métodos psicofísicos quantitativos para avaliar a via magnocelular (FDT, *Frequency Doubling Technology*), parvocelular e koniocelular (*Cambridge Color Test*) e a função das células ganglionares foi avaliada com ERG *pattern*. A espessura da camada de fibras nervosas retinianas foi avaliada por OCT.

Resultados: Observou-se redução da sensibilidade ao contraste acromático (p=0.0298) em doentes com HT, bem como redução da amplitude N95 no PERG (p=0.0499). Os limiares de discriminação cromática estão também aumentados neste grupo (eixos *protan*, *deutan* e *tritan*, p<0.03). Para 80% de especificidade, o FDT mostrou sensibilidade moderada para dano em HT (nasal superior, 66% de sensibilidade). O padrão de declínio está presente todos os testes, mas correlaciona-se melhor com a progressão no OCT ($R_a^2 = 0.47$).

Conclusões: Encontrámos evidência de dano funcional precoce na via magno, parvo e koniocelular desde o grupo de hipertensão ocular. O FDT e O CCT (*protan*) tiveram a melhor *performance* neste aspecto, enquanto que a análise de progressão foi mais consistente com o exame estrutural (OCT). A sensibilidade encontrada é inferior à dos novos testes psicofísicos desenvolvidos pelo nosso grupo (sensibilidade acima de 90%). Os nossos resultados sugerem que o diagnóstico precoce no glaucoma é possível através de testes funcionais de alta sensibilidade com pequenos graus de redundância nas vias visuais.

Palavras-chave: Glaucoma, hipertensão ocular, perimetria estática computadorizada, tomografia de coerência óptica, frequency doubling technology, erg pattern, visão cromática, magnocelular, koniocelular, parvocellular.

INTRODUCTION

Glaucoma is a progressive optic neuropathy characterized by gradual death or dysfunction of retinal ganglion cells (RGC) with subsequent vision loss (Weinreb and Khaw, 2004; Anderson, 2006). Elevated intraocular pressure (IOP) is the main therapeutic target and current treatments aim to reduce IOP to slow vision loss. However, even when the IOP is well-controlled, disease progress may not be halted (European Glaucoma Society, 2017). On the other hand, visual field loss is hard to reliably detect in an early stage, meaning that when clinical features become evident in visual field testing (SAP), RGC loss can be as high as 50-60% (Harwerth et al., 1999; Harwerth and Quigley, 2006).

Taking this into account, current diagnostic techniques do not allow an early diagnosis, therefore jeopardizing possible treatment success. Thus, due to the irreversible RGC loss in glaucoma, it is particularly important that new tests are introduced into clinical practice that enable detection of early defects at a pre-SAP stage. Some studies performed in patients with ocular hypertension, involving psychophysical and electrophysiological tasks, have been conducted in this direction, in order to test their potential

ability to detect early damage (Casson et al., 1993; Johnson et al., 1993; Brusini and Brusatto, 1998; Landers et al., 2000; Sample et al., 2000; Castelo-Branco et al., 2004; Monhart, 2007; Cellini et al., 2012).

To our knowledge, there are very few studies conducted in patients with ocular hypertension to evaluate the diagnostic accuracy of electrophysiological, psychophysical and structural tests simultaneously and their sensitivity to detect early changes (Bach et al., 2006). On the other hand, the ability of those functional and structural tests to monitor disease progression is often overlooked. Patients with ocular hypertension represent an interesting stage, since they are the most recognized at-risk subgroup for developing glaucomatous damage (Bahrami, 2006; Coleman and Miglior, 2008; Kwon et al., 2009).

Ina a previous study, we reported on the development by our group of three novel two-alternative-forced-choice (2AFC) psychophysical discrimination tests (motion, achromatic and chromatic L, M and S cone contrasts), which probe distinct subsets of retinal ganglion cell populations at different disease stages. These testes required the comparison and discrimination of a visual feature (motion, achromatic contrast and chromatic contrast) between two small separated moving single dots (a reference dot and a target dot, which were presented in opposite hemifields), in order to isolate specific ganglion cell populations with a relatively small degree of redundancy (Figure 1). We were able to show very high diagnostic sensitivities (above 90% for 80% specificity) regarding early glaucoma detection (Mateus and Raimundo et al., 2016).

We developed three novel 2AFC psychophysical tests that required the comparison and discrimination of a visual feature (motion, achromatic contrast and chromatic contrast) between two small separated moving single dots (a reference dot and a target dot, which were presented in opposite hemifields), in order to isolate specific ganglion cell populations with a relatively small degree of redundancy (for detailed methodological information and results please refer to Mateus e Raimundo et al., 2016).

In the present study, we aim to characterize early visual impairment in ocular hypertension, glaucoma suspects and primary open glaucoma patients, by means of functional (psychophysical and electrophysiological) and structural methods, using sensitivity analysis. We also aimed to assess the ability of these methods to probe disease progression. For this purpose, we used achromatic contrast sensitivity task using gratings with low spatial/high temporal frequencies (probing magnocellular pathway) (Mateus et al., 2013; Silva et al., 2008), chromatic contrast sensitivity task using a static pattern of circles with a superimposed chromatic C-shaped ring (probing parvo and koniocellular pathways) (Castelo-Branco et al., 2004; Reis et al., 2012), an electrophysiological task assessing retinal ganglion cell (RGC) function (Reis et al., 2012) and optical coherence tomography to detect structural changes in peripapillary RCG axonal layer.

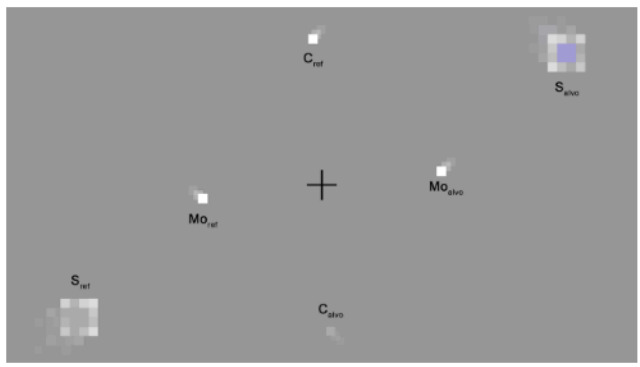

Figure 1 - Schematic illustration of the novel psychophysical tests developed by our group: motion (Mo), achromatic contrast (C), and S-cone chromatic contrast test (S) stimuli, at 0, 90, and 45 degrees meridians with an eccentricity of 7.5, 10, and 15 degrees, respectively. The tests consist of the discriminative comparison of moving dots, a reference dot (ref), and a target dot (trg), which differ on a specific visual attribute—independent variable—being tested (in Mo, a motion/speed difference between dots; in C, a luminance difference and in S, a chrominance, S-cone selective, difference).

METHODS

Patient Selection and Classification

The clinical sample consisted in 52 individuals recruited from the Glaucoma outpatient clinic from our institution: 18 patients with ocular hypertension (HT; n = 18 eyes; mean age ± SD = 62.94 ± 7.38 years; visual acuity (VA) = 0.83 ± 0.16; SAP mean deviation (MD) = -1.00 ± 0.80; cup-to-disc (C/D) diameter = 0.37 ± 0.08), 15 patients diagnosed as glaucoma suspects (GS; n = 15 eyes; mean age ± SD = 65.36 ± 10.85 years; VA = 0.84 ± 0.14; SAP MD = -1.09 ± 0.89; C/D = 0.63 ± 0.07) and 19 patients with established primary open-angle glaucoma (G; n = 19 eyes; mean age ± SD = 71.58 ± 11.48 years; VA = 0.74 ± 0.23; SAP MD = -10.07 ± 7.14; C/D = 0.71 ± 0.09). Patients were compared with an age-matched group of controls (n = 20 eyes; mean age ± SD = 64.45 ± 8.41 years) and normal ancillary testing. Only the dominant eye of each

subject was tested. ANOVA showed no significant age difference between groups.

Patients with primary open-angle glaucoma fulfilled the following criteria: C/D vertical diameter of 0.5 or more, a mean deviation (MD) visual field global index less than -2 dB (or <5% of confidence interval). Glaucoma suspects had C/D of 0.5 or more and normal visual fields (MD more than -2 dB or >5%, of confidence interval). Patients with ocular hypertension showed an elevated intraocular pressure (IOP) of 21 mmHg or more (on at least two occasions), without glaucomatous visual field defects (MD more than -2 dB or >5%, of confidence interval) or optic disc changes (C/D less than 0.5).

All participants underwent a complete ophthalmic examination, including best corrected VA obtained with Snellen chart, Goldmann applanation tonometry (IOP measurement), slit lamp examination of the anterior segment, gonioscopy, retinal examination and optic disc evaluation. All individuals were also submitted to a visual field examination (white-on-white standard automated perimetry, SAP) using the 24-2 standard program of Humphrey automated field analyzer (SITA strategy; HFA II, Carl Zeiss Meditec, Dublin, CA).

Exclusion criteria included the following: neuro-ophthalmologic diseases, retinal diseases, diabetes even in the absence of retinopathy, visual acuity less than 0.6, known color vision disorders, pseudophakic and aphakic eyes, significant media opacities that preclude fundus examination, central corneal thickness outside normal range (540 ± 30 µm), and high ammetropy (sphere > ±4D; cylinder > ±2D).

Frequency-Doubling Technology Perimetry

Frequency-Doubling Technology (FDT) perimeter (Humphrey Matrix perimeter, Welch Allyn, Skaneateles, NY; Zeiss – Humphrey, Dublin, CA) determines achromatic contrast sensitivity measures for detection of sinusoidal gratings with low spatial frequency (0.25 cpd) and high temporal frequency (25Hz) (Turpin et al., 2002; Silva et al., 2008). We performed N-30-F FDT full threshold test, which uses a staircase threshold strategy known as a Modified Binary Search (MOBS) with a four-reversals rule for determining the threshold level (between 0 dB Maximum Contrast and 56 dB Minimum Contrast). Stimulus duration was 300 ms and background luminance was 100 cd/m^2. Stimuli (10° by 10° squares, except for a 5° radius central circular target) were presented at 17 locations, plus 2 nasal locations, testing 30° nasally and 20° temporally.

Subjects were instructed to fixate the black square in the centre of the screen and report the presence of "striped" targets. Performance reliability was assessed by monitoring fixation loss and computing false positive and negative errors (results with false positive/negative errors ≥ 33% and fixation loss ≥ 20% were excluded (Caprioli, 1991; Clement et al., 2009)).

Statistical analysis was performed considering global indices: mean sensitivity (MS), mean deviation (MD) and pattern standard deviation (PSD). For analysis purposes, 4 visual field quadrants (inferior nasal, IN; inferior temporal, IT; superior nasal, SN; superior temporal, ST) and 3 zones were defined: zone 1 corresponds to 5° of visual field, zone 2 contains locations between 5° and 10° eccentricity and zone 3 contains locations between 10° and 20° temporally or 30° nasally.

Cambridge Color Test

We probed chromatic contrast sensitivities using a computer-controlled psychophysical method, the Cambridge Color Test (CCT; Cambridge Research Systems Lda., CRS, Rochester, UK) (Silva et al., 2005; Mateus et al., 2013). This technique uses three parallel, randomly interleaved staircases, corresponding to simultaneous assessment of the three cone confusion axes (protan/red, deutan/green and tritan/blue) modulated in the CIE 1976 u'v' color space (Trivector version of the test). Each staircase was composed by 11 reversals and the mean of the last 7 reversals was taken as the threshold estimate. Subjects looked monocularly at a screen (21-inch monitor; viewing distance - 180cm) with a static pattern of circles of various sizes and luminances with superimposed chromatic contrast defining a Landolt-like C-shaped ring, which forces the subject to use specific color cues. These patches were randomly assigned six different luminance noise levels (8 to 18cd/m^2 in steps of two units). Subjects were instructed to indicate one out of four possible gap positions (up, down, left or right) of the Landolt C stimulus, by pressing one of four buttons of the response box. Psychophysical thresholds were expressed in CIE 1976 u'v' color space units.

Optical Coherence Tomography

We used Spectralis SD-OCT (Heidelberg Engineering, Heidelberg, Germany) to obtain peripapillary RNFL measurements. Image acquisition was performed in high-speed mode, providing an axial resolution of 7 µm and a transversal resolution of 14 µm.

Concerning RNFL measurements, a circular 3.5 mm scan centered on the optic nerve head was used (768 A-scans) and a peripapillary RNFL thickness sectors were evaluated (temporal [315° - 45°], superior [45° - 135°], nasal [135° - 225°], and inferior quadrant [225° - 315°]).

Pattern Electrophysiology

We recorded pattern electroretinogram (PERG; RETIport32, Roland Consult, Germany), which provides information about macular and ganglion cell function, following the ISCEV standards (Bach et al. 2013). DTL fibers were used as recording electrodes. The stimulus consisted in a reversal black and white checkerboard pattern (4.3 reversals per second, rps), with a contrast of 97% and a check size of 0.74°. The stimulus was presented binocularly at a 20-inch monitor (frame rate: 60 Hz), at a viewing distance of 1 meter. When applicable, refractive errors were corrected for the test distance.

The active voltage range of bioelectrical signal was ±100 µV. Signals were amplified with a gain of 100,000 and bandpass filtered (1-100 Hz). We collected 200 artefact-free sweeps to obtain an average waveform (artifact rejection level of 5%). To confirm reproducibility, two PERG measurements were taken. Finally, the amplitudes (µV) and peak time values (ms) of responses for each P-50 and N-95 components and also the PERG ratio (N-95 amplitude/ P-50 amplitude) were analyzed.

Ethics Statement

This study and all procedures were reviewed and approved by the Ethics Commissions of the Faculty of Medicine of the University of Coimbra ("Comissão de Ética da Faculdade de Medicina da Universidade de Coimbra") and were conducted in accordance with the Declaration of Helsinki. Written informed consent was obtained from each participant and procedures of the study were fully explained.

Statistical Analysis

Statistical analysis was performed using SPSS statistical software package (IBM SPSS Statistics 24, IBM Corporation, NY, USA). After verifying the normality of the data across the study groups (Kolmogorov-Smirnov normality test and Levene homogeneity test), we applied a parametric analysis for overall means comparisons [multivariate analysis of variance (ANOVA)] and Fisher HSD post-hoc test for multiple comparisons. Spearman coefficient was used to correlate each quantitative test parameter and ordered subject grouping categories. When applicable, functional and structural data was fit with linear regression model and the adjusted coefficient of determination (R^2_a) was used as an indicator of goodness of fit.

The Receiver Operating Characteristic (ROC) curve analyses were performed using MedCalc version 12.2.1.0 (MedCalc Software, Mariakerke, Belgium) to determine sensitivities at a fixed specificity (approximately 80%). Since the classification of patients was based on the results of SAP and optic nerve head excavation, these two parameters were not used to compare sensitivities.

The relative diagnostic accuracies were assessed by comparing areas under the ROC curves (AUC). Results with $p<0.05$ were considered statistically significant.

RESULTS

Frequency-Doubling Technology Perimetry

We found a significant group effect on mean contrast sensitivity, MS [$F_{(3,75)} = 23.86$, $p<0.0001$], mean deviation, MD [$F_{(3,75)} = 20.22$, $p<0.0001$] and pattern standard deviation [$F_{(3,75)} = 12.23$, $p<0.0001$]. For MS and MD, post-hoc tests (corrected for multiple comparisons) revealed significant differences between all groups ($p<0.04$), except for HT vs GS (see Figure 2 and Figure 3A for a representative example); for PSD, post-hoc tests showed only significant differences between C and G ($p<0.0001$), HT and G ($p<0.0001$), GS and G ($p=0.0001$).

Furthermore, a moderate correlation between MS and ordered subject grouping categories was found (MS: Rho = -0.542, $p<0.0001$), whereby CS performance declines with ordered levels of glaucoma progression. We also found moderate correlations between MD/PSD and clinical stages (MD: Rho = -0.585, $p<0.0001$;

PSD: Rho = 0.510, p<0.0001). Then, we applied a linear regression to data to investigate the presence of linear trends and using this approximation found that mean CS decreases linearly 3.26 dB per clinical stage [MS: *y=33.26-3.26*clinical stage*, F(1,77) = 52.87, R^2_a = 0.40, p<0.0001; MD: *y=9.37-4.56*clinical stage*, F(1,77) = 33.14, R^2_a = 0.39, p<0.0001; PSD: *y=2.41+0.97*clinical stage*, F(1,77) = 26.87, R^2_a = 0.25, p<0.0001]. We also studied the effect of disease progression in terms of eccentricity and its loss was around 3.41/3.58 dB per clinical stage for the most central locations [Zone 1: *y=35.95-3.41*clinical stage*, F(1,77) = 39.25, R^2_a = 0.33, p<0.0001; Zone 2: *y=34.89-3.58*clinical stage*, F(1,77) = 50.53, R^2_a = 0.39, p<0.0001] and was less pronounced in the most peripheral location, around 3.16 dB [Zone 3: *y=32.60-3.16*clinical stage*, F(1,77) = 48.95, R^2_a = 0.39, p<0.0001]. Along visual field quadrants, CS decreases between 2.94 dB and 3.77 dB per clinical stage [ST: *y=33.65-3.77*clinical stage*, F(1,77) = 61.19, R^2_a = 0.44; SN: *y=33.01-3.33* clinical stage*, F(1,77) = 35.74, R^2_a = 0.31; IN: *y=32.69-3.02*clinical stage*, F(1,77) = 39.54, R^2_a = 0.33; IT: *y=33.22-2.94*clinical stage*, F(1,77) = 37.40, R^2_a = 0.32; p<0.0001 for all cases].

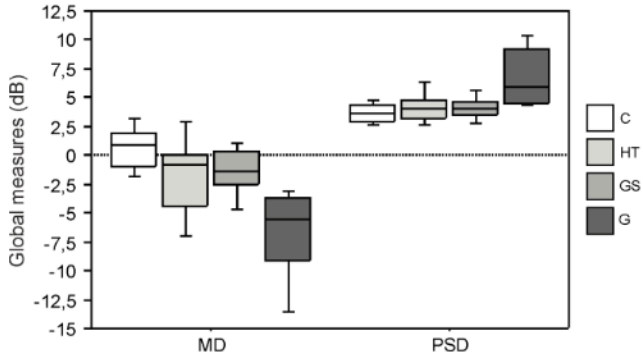

Figure 2 - Achromatic contrast sensitivity, expressed in FDT global measures (MD – mean deviation; PSD – pattern standard deviation), along the disease progression stages (control, C; ocular hypertensive, HT; glaucoma suspect, GS; and glaucoma, G). Bars depict 10th and 90th percentiles, the *top* and *bottom borders* of the boxes represent the 25th and 75th percentiles, and the *line* segment *inside* the boxes depicts the median.

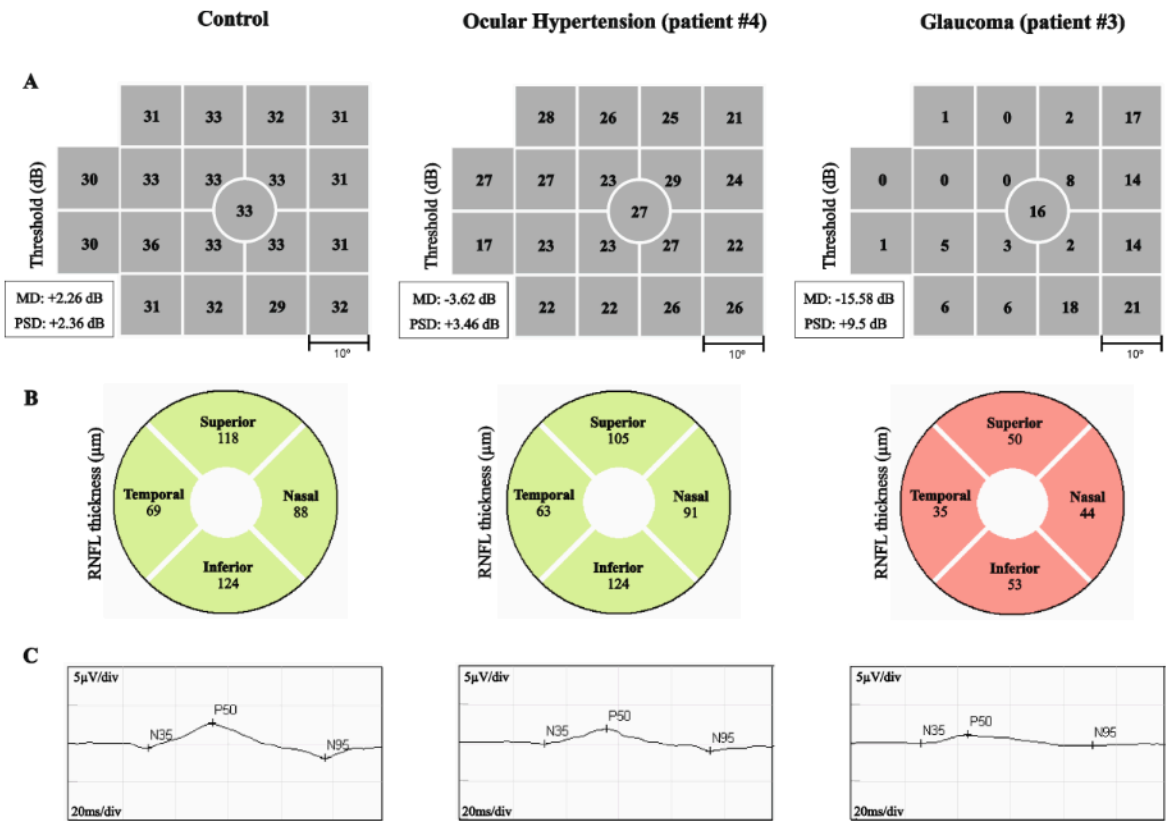

Figure 3 - FDT perimetry output (A), OCT – peripapillary RNFL thickness map (B) and PERG plots (C) of representative control, ocular hypertensive (#4) and glaucoma (#3) cases. Note the progressive impairment in all measures with disease progression, except for peripapillary RNFL thickness that showed no differences between the control subject and ocular hypertensive patient.

Cambridge Color Test

We found a significant group effect on chromatic contrast sensitivity, CS for protan (red) [$F_{(3,72)}$ = 4.485, p=0.0061], deutan (green) [$F_{(3,72)}$ = 4.401, p=0.0067] and tritan (blue) [$F_{(3,72)}$ = 7.055, p=0.0003] cone confusion axes. Concerning post-hoc tests, we found significant differences between C and HT (p<0.03), C and G (p<0.001), HT and G (p<0.008), GS and G (p<0.02), for all chromatic axes (Figure 4).

Using Spearman correlation analysis, a significant correlation between chromatic thresholds and ordered subject grouping categories was found (protan: Rho = 0.598; deutan: Rho = 0.594; tritan: Rho = 0.658; p<0.0001). This means that chromatic thresholds increase with disease progression. Note that high chromatic thresholds relate to low CS. In this sense, through the linear regression analysis we found that chromatic thresholds increase linearly (corresponding to a contrast sensitivity decline) 37.86, 38.96 and 51.63 u'v' units per clinical stage, for protan, deutan and tritan axes, respectively [Protan: *y=-3.84+37.86*clinical stage*, F(1,74) = 10.22, R^2_a = 0.11, p=0.002; Deutan: *y=-5.27+38.96*clinical stage*, F(1,74) = 10.61, R^2_a = 0.11, p=0.0017; Tritan: *y=4.31+51.63*clinical stage*, F(1,74) = 18.10, R^2_a = 0.19, p<0.0001].

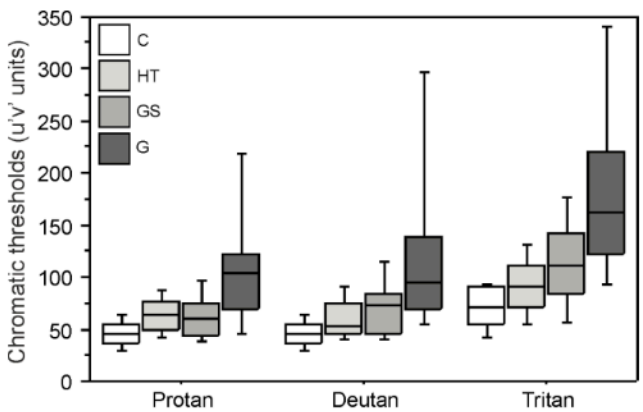

Figure 4 - Chromatic contrast sensitivity performance over clinical stages (control, C; ocular hypertensive, HT; glaucoma suspect, GS; and glaucoma, G). Note that higher chromatic thresholds are related to lower contrast sensitivity.

Optical Coherence Tomography

We found a significant effect of group on peripapillary RNFL thickness for superior [$F_{(3,75)}$ = 23.73, p<0.0001], inferior [$F_{(3,75)}$ = 23.25, p<0.0001], nasal [$F_{(3,75)}$ = 12.59, p<0.0001] and temporal [$F_{(3,75)}$ = 19.97, p<0.0001] quadrants. Post-hoc tests showed significant differences between all clinical stages (p<0.04), except for C vs HT (p>0.05), for all tested RNFL quadrants (Figure 5; see also a representative example in Figure 3B).

We also found a significant correlation between RNFL thickness and ordered subject grouping categories (superior: Rho = -0.706; inferior: Rho = -0.649; nasal: Rho = -0.515; temporal: Rho = -0.655; p<0.0001), which means that peripapillary RNFL thickness decreases with the glaucoma progression. Thus, RNFL thickness decreases linearly with disease progression around 13.14 µm per clinical stage for superior quadrant [*y=137.29-13.14*clinical stage*, F(1,77) = 69.69, R^2_a = 0.47, p<0.0001], 15.06 µm for inferior [*y=152.09-15.06*clinical stage*, F(1,77) = 64.48, R^2_a = 0.45, p<0.0001], 7.11 µm for nasal [*y=85.83-7.11*clinical stage*, F(1,77) = 29.61, R^2_a = 0.27, p<0.0001] and 6.92 µm for temporal quadrants [*y=78.70-6.92*clinical stage*, F(1,77) = 54.59, R^2_a = 0.41, p<0.0001].

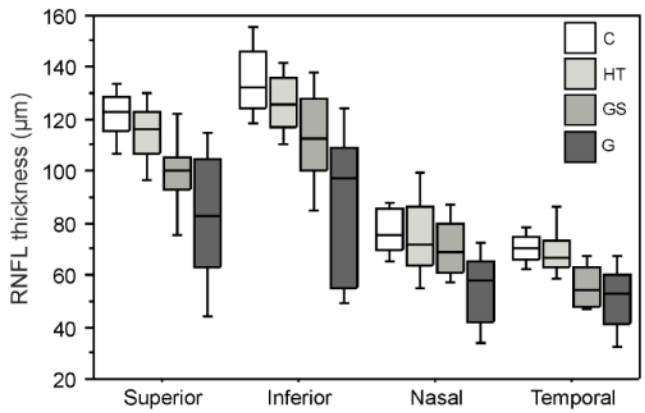

Figure 5 - Peripapillary RNFL thickness assessed by SD-OCT across disease progression stages (control, C; ocular hypertensive, HT; glaucoma suspect, GS; and glaucoma, G).

Pattern Electroretinogram

We found a significant group effect on amplitudes of P-50 [$F_{(3,67)}$ = 7.67, p=0.0002] and N-95 [$F_{(3,67)}$ = 10.57, p<0.0001] waves. This effect was not verified for the implicit time of both waves, as well as N-95/P-50 ratio. Post-hoc tests for multiple comparisons revealed the following significant differences: $P\text{-}50_{amplitude}$ – C vs GS (p=0.0233), C vs G (p<0.0001), HT vs G (p=0.0025), GS vs G (p=0.0541); and for $N\text{-}95_{amplitude}$ – C vs HT (p=0.0499), C vs GS (p=0.0005), C vs G (p<0.0001), HT vs G (p=0.0019) (see Figure 6 and a representative example in Figure 2C).

Spearman correlation analysis showed that P-50 and N-95 waves amplitudes decrease moderately with the disease progression (P-50 wave: Rho = -0.487; N-95 wave: Rho = -0.524; p<0.0001). This amplitude decrease occurs in a linear fashion around 0.29 µV per clinical stage for the P-50 wave and 0.487 µV for the N-95 wave [P-50: *y=2.71-0.29*clinical stage*, F(1,69) = 23.20, R^2_a = 0.24, p<0.0001; N-95: *y=3.75-0.49*clinical stage*, F(1,69) = 32.35, R^2_a = 0.31, p<0.0001].

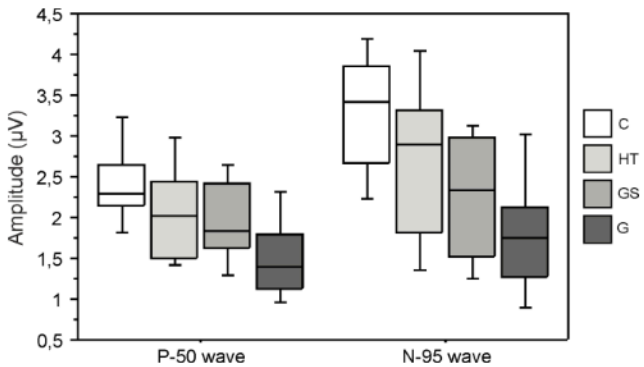

Figure 6 - Amplitude of P-50 and N-95 waves of pattern ERG over clinical stages (control, C; ocular hypertensive, HT; glaucoma suspect, GS; and glaucoma, G).

Correlation analysis

We found significant correlations between structural and functional measures specifically for the *glaucoma group*: 1) Peripapillary RNFL thickness (superior quadrant) correlated positively with PERG N-95 wave amplitude (r=0.560, p=0.0115), FDT MD (r=0.640, p=0.0086), FDT Ring 1 (r=0.588, p=0.0195) and FDT Ring 2 (r=0.547, p=0.0333); 2) Peripapillary RNFL thickness (inferior quadrant) correlated positively with FDT MD (r=0.514, p=0.0492) and FDT Ring 1 (r=0.537, p=0.0376). We also found a positive correlation between PERG N-95 wave amplitude and FDT in the inferior temporal quadrant (r=0.528, p=0.0419). These correlation patterns were not found in HT, GS and control groups.

ROC Curve – Sensitivity/Specificity analysis

ROC curves were generated for all included tests in order to compare sensitivities at a fixed specificity (approximately 80%). For *control vs ocular hypertensive* analysis, at approximately 80% specificity, the highest sensitivity value was found for FDT SN quadrant (66%; cut-off: 26.6 dB), followed by CCT Protan (56%; cut-off: 59 u'v' units) (for more details see Table 1A).

Concerning *ocular hypertensive vs glaucoma* analysis, the highest sensitivity values were found for FDT ST quadrant (93%; cut-off: 22.75 dB), FDT Zone 2 (87%; cut-off: 23 dB) and CCT Tritan (84%; cut-off: 115 u'v' units) (see Table 1B). On the other hand, for *control vs glaucoma* analysis, we found sensitivities higher than 80% (at approximately 80% specificity) for all parameters, except for PERG waves implicit time and ratio (around 20-30%).

Diagnostic accuracy by Areas Under the ROC Curve

The AUC is an important measure that summarizes the diagnostic accuracy of each parameter. An AUC equal to 1 represents a perfect discrimination between groups, whereas an AUC of 0.5 represents chance discrimination. In *control vs ocular hypertensive* analysis, we found AUC values between 0.777 and 0.519. The higher AUC values correspond to CCT Protan (AUC = 0.777, p=0.0002), CCT Tritan (AUC = 0.729, p=0.0054) and also FDT IN quadrant (AUC = 0.700, p=0.0190) (Table 1A).

On the other hand, in *ocular hypertensive vs glaucoma* analysis we found AUC values between 0.924 and 0.506. In this sense, FDT ST quadrant (AUC = 0.924), OCT RNFL inferior (AUC = 0.901) and OCT RNFL superior (AUC = 0.883) showed the higher AUC values (p<0.0001) (see Table 1 B). Concerning *control vs glaucoma* analysis, the parameter that showed the higher AUC was FDT MD (AUC = 0.971, p<0.0001). The AUC values were higher than 0.892 for all parameters (p<0.0001), except for PERG waves implicit time and ratio that represent only a change discrimination between groups (AUC values between 0.514 and 0.504).

Table 1 - Areas under the receiver operating characteristic (ROC) curve (AUC) and associated 95% confidence interval (CI) are presented for psychophysical, electrophysiological and structural tests. Sensitivities obtained for each parameter at ~80% specificity, and criterion values used for that specificity are also presented [(A) Control vs Ocular hypertensive analysis; (B) Ocular hypertensive vs Glaucoma analysis].

A

Parameters	AUC	95% CI	P value	Sensitivity/ Specificity (%)	Criteria for 80% Specificity
FDT perimetry					
MS	0.684	0.537, 0.808	0.0307	44/81	26.63
MD	0.694	0.547, 0.816	0.0253	50/81	-1.08
PSD	0.597	0.449, 0.733	n.s.	28/81	4.34
Zone 1	0.635	0.486, 0.766	n.s.	39/81	29
Zone 2	0.629	0.481, 0.762	n.s.	39/81	27.25
Zone 3	0.693	0.546, 0.815	0.0231	44/81	26.21
ST quadrant	0.615	0.467, 0.750	n.s.	50/81	26.75
SN quadrant	0.677	0.530, 0.802	0.0416	66/81	26.6
IN quadrant	0.700	0.554, 0.821	0.0190	44/81	27
IT quadrant	0.633	0.485, 0.765	n.s.	33/81	26.5
Cambridge color test					
Protan	0.777	0.624, 0.889	0.0002	56/80	59
Deutan	0.676	0.516, 0.810	0.0355	44/80	55.1
Tritan	0.729	0.572, 0.853	0.0054	50/80	91.9
OCT – RNFL thickness					
Superior	0.642	0.489, 0.770	n.s.	34/82	114
Inferior	0.653	0.498, 0.787	n.s.	28/82	121
Nasal	0.569	0.415, 0.714	n.s.	33/79	66
Temporal	0.620	0.465, 0.759	n.s.	33/82	63
PERG					
P-50 amplitude	0.663	0.491, 0.807	n.s	39/80	2.05
N-95 amplitude	0.671	0.500, 0.814	0.0509	45/80	2.39
P-50 implicit time	0.547	0.378, 0.709	n.s.	28/80	53
N-95 implicit time	0.607	0.436, 0.761	n.s.	39/80	93
N-95/P-50 ratio	0.519	0.352, 0.684	n.s.	22/80	1.06

Note: FDT = frequency doubling technology; MS = mean sensitivity; MD = mean deviation; PSD = pattern standard deviation; ST = superior temporal; SN = superior nasal; IN = inferior nasal; IT = inferior temporal; OCT = optical coherence tomography; RNFL = retinal nerve fiber layer; PERG = pattern electroretinogram; n.s. = not significant.

B

Parameters	AUC	95% CI	P value	Sensitivity/ Specificity (%)	Criteria for 80% Specificity
FDT perimetry					
MS	0.841	0.672, 0.944	<0.0001	73/83	21.16
MD	0.807	0.633, 0.923	0.0001	60/83	-5.09
PSD	0.837	0.667, 0.942	<0.0001	67/83	4.85
Zone 1	0.844	0.676, 0.947	<0.0001	80/83	26
Zone 2	0.870	0.708, 0.961	<0.0001	87/83	23
Zone 3	0.824	0.652, 0.934	<0.0001	67/83	20.29
ST quadrante	0.924	0.777, 0.987	<0.0001	93/83	22.75
SN quadrante	0.783	0.606, 0.907	0.0005	60/83	21.2
IN quadrante	0.785	0.608, 0.908	0.0004	53/83	20
IT quadrante	0.833	0.663, 0.940	<0.0001	73/83	23
Cambridge color test					
Protan	0.814	0.652, 0.923	<0.0001	74/83	77
Deutan	0.835	0.676, 0.936	<0.0001	68/83	79
Tritan	0.857	0.702, 0.950	<0.0001	84/83	115
OCT – RNFL thickness					
Superior	0.883	0.735, 0.965	<0.0001	74/83	102
Inferior	0.901	0.757, 0.974	<0.0001	79/83	114
Nasal	0.832	0.673, 0.934	<0.0001	68/83	61
Temporal	0.851	0.695, 0.946	<0.0001	79/83	60
PERG					
P-50 amplitude	0.754	0.585, 0.881	0.0017	53/83	1.14
N-95 amplitude	0.754	0.585, 0.881	0.0018	53/83	1.74
P-50 implicit time	0.506	0.337, 0.674	n.s.	37/83	56
N-95 implicit time	0.601	0.427, 0.758	n.s.	26/83	96
N-95/P-50 ratio	0.596	0.423, 0.754	n.s.	32/83	0.934

DISCUSSION

In this study we have characterized the early visual impairment of patients with ocular hypertension, using psychophysical, electrophysiological and structural methods. We found changes in achromatic and chromatic contrast sensitivities and also in RGC function even in the ocular hypertensive stage, corroborating the notion that functional damage assessed by sensitive methods may precede structural and functional (SAP) damage detected by current diagnostic techniques (Ventura et al., 2006). According, a significant correlation between structural and functional damage was found, but only in the later stages of the disease.

In this sense, visual performance seems to be impaired even before the appearance of visual field defects in standard automated perimetry (SAP) and also structural changes in optic nerve head and RNFL. This evidence is consistent with some previous studies in ocular hypertension, which use functional methods to indirectly assess specific RGC populations (Casson et al., 1993; Johnson et al., 1993; Brusini and Brusatto, 1998; Landers et al., 2000; Castelo-Branco et al., 2004; Bach et al., 2006; Cellini et al., 2012).

We also found that functional and structural measures correlated significantly and moderately with the stage of the ordered clinical categories corresponding to the natural history of the disease, making these tests potential markers of disease progression. In general, the pattern of decline is approximately linear and is more pronounced for structural tests, namely RNFL thickness. About 47% of variability in RNFL thickness is explained by disease progression ($R_a^2 = 0.47$), showing the role of this test in monitoring the progression of glaucoma.

Visual performance within multiple visual channels was tested using a computerized chromatic contrast sensitivity test to probe parvo and koniocellular pathways and a FDT perimetry to probe magnocellular pathway (Silva et al., 2005; Ribeiro et al., 2012; Mateus et al., 2013). We found a relative

damage of all retinocortical pathways since the initial hypertensive stage of the disease, proving that glaucoma is not restricted to impairment of the mangocellular pathway (Kalloniatis et al., 1993; Felius et al., 1995; Greenstein et al., 1996; Alvarez et al., 1997; Castelo-Branco et al., 2004), an historical and, in our opinion, outdated notion.

Concerning ROC curve analyses, we found that FDT (superior nasal quadrant) showed the highest sensitivity value (66%) for 80% specificity. This perimetry uses high temporal/low spatial frequency stimuli, which functionally isolated a specific subgroup of magnocellular ganglion cells (My cells) (Quigley, 1998), increasing its sensitivity to detect glaucomatous defects before SAP. On the other hand, PERG waves amplitude showed a low sensitivity to detect early functional damage, which do not exceed 45% for 80% specificity, possibly due to this test study macular function, whereas the initial glaucomatous impairment appears in the peripheral visual field (Quigley, 2011). Interestingly, our novel psychophysical discrimination tests (probing motion sensitivity and achromatic and chromatic contrast sensitivities) (Mateus and Raimundo et al., 2015), which were applied to the same sample, showed a larger sensitivity to detect functional damage at the ocular hypertensive stage (above 90% for 80% specificity, reaching 100% in some cases). These novel tests exhibit a higher sensitivity when compared with the FDT, PERG and CCT, suggesting that tests with a smaller degree of redundancy across pathways enable for a greater diagnostic accuracy.

CONCLUSION

FDT and CCT Protan performed well in detecting early glaucomatous damage even in a cohort of patients with ocular hypertension (normal SAP and normal OCT RFNL), whereas longitudinal analysis using OCT for RFNL changes appears to be the best method to monitor the progression of the glaucomatous disease. We have also shown that glaucomatous damage is rather unselective, with damage seen in all main visual pathways (magnocellular, parvocellular and koniocellular), contrary to prior beliefs of selective magnocellular impairment. Based on these tests results and our previous results with novel psychophysical tests, we believe early diagnosis in glaucoma is possible by exploiting visual pathways with a small degree of redundancy through high sensitivity functional tests.

REFERENCES

1. Alvarez S, Pierce G, Vingrys A, Benes S, Weber P, King-Smith P (1997) Comparison of red-green, blue-yellow and achromatic losses in glaucoma. Vision Res; 37: 2295-2301.
2. Anderson RS (2006) The psychophysics of glaucoma: improving the structure/function relationship. Prog Retin Eye Res; 25: 79-97.
3. Bach M, Brigell MG, Hawlina M, Holder GE, Johnson MA, McCulloch DL, Meigen T, Viswanathan S (2013) ISCEV standard for clinical pattern electroretinography (PERG): 2012 update. Doc Ophthalmol 126:1-7.
4. Bach M, Unsoeld AS, Philippin H, Staubach F, Maier P, Walter HS, Bomer TG, Funk J (2006) Pattern ERG as an early glaucoma indicator in ocular hypertension: a long-term, prospective study. Invest Ophthalmol Vis Sci; 47: 4881-4887.
5. Bahrami H (2006) Causal inference in primary open angle glaucoma: specific discussion on intraocular pressure. Ophthalmic Epidemiol; 13: 283-289.
6. Brusini P, Busatto P (1998) Frequency doubling perimetry in glaucoma early diagnosis. Acta Ophthalmol Scand Suppl; 23-24.
7. Caprioli J (1991) Automated perimetry in glaucoma. Am J Ophthalmol; 111: 235-239.
8. Casson EJ, Johnson CA, Shapiro LR (1993) Longitudinal comparison of temporal-modulation perimetry with white-on-white and blue-on-yellow perimetry in ocular hypertension and early glaucoma. J Opt Soc Am A Opt Image Sci Vis; 10: 1792-1806.
9. Castelo-Branco M, Faria P, Forjaz V, Kozak LR, Azevedo H (2004) Simultaneous comparison of relative damage to chromatic pathways in ocular hypertension and glaucoma: correlation with clinical measures. Invest Ophthalmol Vis Sci; 45: 499-505.
10. Cellini M, Toschi PG, Strobbe E, Balducci N, Campos EC (2012) Frequency doubling technology, optical coherence technology and pattern electroretinogram in ocular hypertension. BMC Ophthalmol; 12: 33.
11. Clement CI, Goldberg I, Healey PR, Grahams (2009) Humphrey matrix frequency doubling perimetry for detection of visual-field defects in open-angle glaucoma. Br J Opthalmol; 93: 582-588.
12. Coleman AL, Miglior S (2008) Risk factors for glaucoma onset and progression. Surv Ophtalmol; 53: S3-S10.
13. European Glaucoma Society Terminology and Guidelines for Glaucoma, 4th Edition - Chapter 3: Treatment

principles and optionsSupported by the EGS Foundation: Part 1: Foreword; Introduction; Glossary; Chapter 3 Treatment principles and options. Br J Ophthalmol. 2017;101(6):130-195.
14. Felius J, deJong LAMS, van den Berg TJTP, Greve EL (1995) Functional characteristics of blue-on-yellow perimetric thresholds in glaucoma. Invest Ophthalmol Vis Sci; 36: 1665-1674.
15. Greenstein VC, Halevy D, Zaidi Q, Koenig KL, Ritch RH (1996) Chromatic and luminance system deficits in glaucoma. Vision Res; 36: 621-629.
16. Harwerth R S, Carter-Dawson L, Shen F, Smith 3rd E L, Crawford M L (1999) Ganglion cell losses underlying visual field defects from experimental glaucoma. Invest Ophthalmol Vis Sci; 40: 2242-2250.
17. Harwerth R S, Quigley H A (2006) Visual field defects and retinal ganglion cell losses in patients with glaucoma. Arch Ophthalmol; 124: 853-859.
18. Johnson CA, Adams AJ, Casson EJ, Brandt JD (1993) Blue-on-yellow perimetry can predict the development of glaucomatous visual field loss. Arch Ophthalmol; 111: 645-650.
19. Kalloniatis M, Harwerth RS, Smith EL, De Santis L (1993) Colour vision anomalies following experimental glaucoma in monkeys. Ophthalmic Physiol Opt; 13: 56-67.
20. Kwon YH, Fingert JH, Kuehn MH, Alward WL (2009) Primary open-angle glaucoma. N Engl J Med; 360: 1113-1124.
21. Landers J, Goldberg I, Graham S (2000) A comparison of short wavelength automated perimetry with frequency doubling perimetry for early detection of visual field loss in ocular hypertension. Clin Experiment Ophthalmol; 28: 248-252.
22. Mateus C, Lemos R, Silva MF, Reis A, Fonseca P, Oliveiros B, Castelo-Branco M (2013) Aging of low and high level vision: from chromatic and achromatic contrast sensitivity to local and 3D object motion perception. PLoS One 8:e55348.
23. Mateus C, Raimundo M, Oliveiros B, Faria P, Reis A, Castelo-Branco M. A New Approach to Assess Early Progressive Loss Across Multiple Visual Channels In the Natural History of Glaucoma. J Glaucoma. 2016;25(6):e581-90.
24. Monhart M (2007) What are the options of psychophysical approaches in glaucoma? Surv Ophthalmol; 52: S127-S133.
25. Quigley HA (1998) Identification of glaucoma-related visual field abnormality with screening protocol of frequency doubling technology. Am J Ophthalmol; 125: 819-829.
26. Quigley HA (2011) Glaucoma. Lancet; 377: 1367-1377.
27. Reis A, Mateus C, Viegas T, Florijn R, Bergen A, Silva E, Castelo-Branco M (2013) Physiological evidence for impairment in autosomal dominant optic atrophy at the pre-ganglion level. Graefes Arch Clin Exp Ophthalmol 251:221-234.
28. Ribeiro MJ, Violante IR, Bernardino I, Ramos F, Saraiva J, Reviriego P, Upadhyaya M, Silva ED, Castelo-Branco M (2012) Abnormal achromatic and chromatic contrast sensitivity in neurofibromatosis type 1. Invest Ophthalmol Vis Sci; 53: 287-293.
29. Sample PA, Bosworth CF, Blumenthal EZ, Girkin C, Weinreb RN (2000) Visual function-specific perimetry for indirect comparison of different ganglion cell populations in glaucoma. Invest Ophthalmol Vis Sci; 41: 1783-1790.
30. Silva MF, Faria P, Regateiro FS, Forjaz V, Januário C, Freire A, Castelo-Branco M (2005) Independent patterns of damage within magno-, parvo- and koniocellular pathways in Parkinson's disease. Brain 128:2260-2271.
31. Silva MF, Maia-Lopes S, Mateus C, Guerreiro M, Sampaio J, Faria P, Castelo-Branco M (2008) Retinal and cortical patterns of spatial anisotropy in contrast sensitivity tasks. Vision Res; 48: 127-135.
32. Turpin A, McKendrick A, Johnson C, Vingrys A (2002a) Performance of efficient test procedures for frequency-doubling technology perimetry in normal and glaucomatous eyes. Invest Ophthalmol Vis Sci; 43: 709-715.
33. Ventura LM, Sorokac N, De Los Santos R, Feuer WJ, Porciatti V (2006) The relationship between retinal ganglion cell function and retinal nerve fiber thickness in early glaucoma. Invest Ophthalmol Vis Sci; 47: 3904-3911.
34. Weinreb RN, Khaw PT (2004) Primary open-angle glaucoma. Lancet; 363: 1711-1720.

CONTACT

Miguel Raimundo
mglraimundo@gmail.com

Ophthalmology Department, Centro Hospitalar e Universitário de Coimbra, Coimbra (CHUC), Portugal.